Journal of Photochemistry and Photobiology A: Chemistry 223 (2011) 111–118

Contents lists available at SciVerse ScienceDirect

Journal of Photochemistry and Photobiology A: Chemistry

journal homepage: www.elsevier.com/locate/jphotochem

Water soluble 1,8-naphthalimide fluorescent pH probes and their application to bioimagings

Jian Xie [a], Yuhua Chen [b], Wen Yang [a], Dongmei Xu [a,*], Keda Zhang [a]

[a] National Engineering Laboratory for Modern Silk, Key Laboratory of Organic Synthesis of Jiangsu Province, Jiangsu Key Laboratory of Advanced Functional Polymer Design and Application, College of Chemistry, Chemical Engineering and Materials Science, Soochow University, Suzhou 215123, China
[b] College of Pre-clinical Medical and Biological Science, Soochow University, Suzhou 215123, China

ARTICLE INFO

Article history:
Received 20 April 2011
Received in revised form 8 August 2011
Accepted 13 August 2011
Available online 22 August 2011

Keywords:
Naphthalimide
Fluorescence
Probe
Proton
Bioimaging

ABSTRACT

Two water soluble and high selective 1,8-naphthalimide fluorescent probes for protons have been synthesized by simple and efficient one-step reaction under very mild conditions. Their photophysical characteristics in Britton–Robinson buffer have been studied. All detections were carried out in aqueous media and a large number of biologically relevant ions showed no obvious interferences with the detection. Fluorescent imaging of living cells treated with the probe in different pH media indicated that the probe could provide extracelluar pH information by the cell's fluorescence.

1. Introduction

Intracellular pH (pH_i) and extracelluar pH (pH_e) play many critical roles in cell, enzyme, and tissue activities because they are closely related to the physiological process of cells and organelles [1–4]. Monitoring pH changes inside and outside living cells is therefore very important for studying cellular internalization pathways and extracelluar environments, as well as diagnosing and removing diseases [5–8]. Among several cellular pH measurement methods, fluorescent probe techniques are extensively used owing to the great advantages of operational simplicities, high sensitivities, no destruction to cells and in situ and real-time observation of pH changes [2]. Many fluorescent probes for monitoring pH value at the cellular level have been reported, such as the fluorescein-based dyes (including the most widely used BCECF: 2′,7′-bis(2-carboxyethyl)-5-(and -6)-carboxyfluorescein) [9–11], benzoxanthene dyes (including the *second* most widely used C.SNARF-1: 5-(and -6)-carboxy-seminaphthorhodafluor-1) [12–14], 1,8-naphthalimide dyes [15,16], anthracene dyes [17–19], cyanine-based dyes [1,20–24], BODIPY-based dyes [25–28], rhodamine-based dyes [29] and nanoparticles [30–32]. Most of them were used to detect pH_i. The pH_i fluorescent probes have made great contributions to the study of vital movement and nosogenesis. However, some problems still exist, for example, the solubility, cell membrane permeability, photobleaching, cytotoxicity of the dyes, and the leakage of the dyes from cells [2]. Moreover, pH_e fluorescent probes are rarely reported. Therefore, new fluorescent probes for pH_i and pH_e measurement are highly desirable [29].

1,8-naphthalimide (Naph) is among the most frequently used signaling fragments in the synthesis of fluorescent probes [33–39]. The Naph derivatives have not only high quantum yield and good photostability but also favourable compatibility and high selectivity by adjusting the substituents connected to the N-atom of the imide fragment and the 4,5- or 3,4-position of the Naph moiety. The Naph has widely been exploited in the design of photoinduced electron transfer (PET) probes and the receptors were mostly tertiary amines [40,41]. N,N-dimethylethylenediamine (DMEDA) and N,N-diethylethylenediamine (DEEDA) are two of the typical receptor-providers which can readily introduce (2-(dimethylamino)ethyl)amino (DMAEA) and (2-(diethylamino)ethyl)amino (DEAEA) units to the Naph and provide dimethylamino (DMA) and diethylamino (DEA) receptors. The commercial LysoSensor green DND-153 for pH_i measurement has DMA as its receptor [42], other probes with DMA or DEA receptors are reported sensitive to Cr^{3+}, Fe^{3+} and H^+ [43]. The pH detections with this kind of probes in the literature are generally troubled with the insufficient water solubility of the probes and the interference from the coexist cations [44–47]. Herein, we report two water soluble and high selective fluorescent pH probes from

* Corresponding author. Tel.: +86 0512 65882027.
E-mail address: xdm.sd@163.com (D. Xu).

1010-6030/$ – see front matter © 2011 Elsevier B.V. All rights reserved.
doi:10.1016/j.jphotochem.2011.08.006

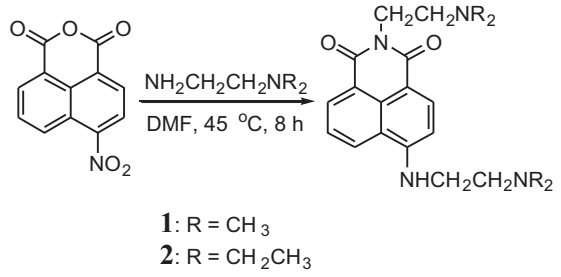

Scheme 1. Synthesis of probes **1** and **2**.

1,8-naphthalimide and DMAEA (or DEAEA), and their application in fluorescent imaging of living cells at different pH_e.

2. Experimental

The intermediate 4-nitronaphthalic anhydride was prepared according to the literature [48]. Probe **1** and probe **2** were synthesized by one step reaction between 4-nitro-1,8-naphthalic anhydride and DMEDA (or DEEDA) under very mild conditions (Scheme 1), which is simpler and more efficient than the literature methods [49,50]. Probe **1** was used as a potential DNA-binding antitumor agent in the literature [49] and probe **2** was used for the repair of meniscal lesions in the literature [50].

2.1. Synthesis of probe *1*

2-(2-(dimethylamino)ethyl)-6-((2-(dimethylamino)ethyl) amino)-1H-benzo[de]isoquinoline-1,3(2H)-dione (**1**): To a solution of 4-nitro-1,8-naphthalic anhydride (0.2 g, 822 μM) in N,N-dimethylformamide (3 mL), N,N-dimethylethylenediamine (1.2 mL, 11 mM) was added dropwise at room temperature. The solution was stirred for 8 h at 45 °C, then, the solvent was removed under reduced pressure. Silica gel chromatography (methanol/chloroform, volume ratio 1/30) afforded 0.22 g of **1**. Yield: 75.0%. m.p. 119–121 °C. IR (KBr, cm^{-1}): 3418.5, 2943.6, 2837.4, 1682.2, 1641.4. ^1H NMR ($CDCl_3$, 400 MHz) δ (ppm): 2.34 (s, 6H), 2.38 (s, 6H), 2.66 (t, 2H, J = 12.0 Hz), 2.74 (t, 2H, J = 12.0 Hz), 3.38 (m, 2H), 4.32 (t, 2H, J = 14.4 Hz), 6.31 (s, 1H), 6.66 (d, 1H, J = 8.0 Hz), 7.62 (t, 1H, J = 8.0 Hz), 8.14 (d, 1H, J = 8.0 Hz), 8.45 (d, 1H, J = 8.0 Hz), 8.57 (d, 1H, J = 7.2 Hz). ^{13}C NMR ($CDCl_3$, 300 MHz) δ (ppm): 38.04, 40.32, 45.28, 45.98, 57.07, 57.27, 104.55, 110.06, 120.50, 123.05, 124.75, 126.68, 129.97, 131.30, 134.77, 149.87, 164.34, 164.95. LC-MS: m/z 355.2 $(M+H)^+$. Elementary analysis: $C_{20}H_{26}N_4O_2$ (354.2); Calcd (%): C 67.77, H 7.39, N 15.81, found (%): C 67.38, H 7.27, N 15.46.

2.2. Synthesis of probe *2*

2-(2-(diethylamino)ethyl)-6-((2-(diethylamino)ethyl)amino)-1H-benzo[de]isoquinoline-1,3(2H)-dione (**2**): To a solution of 4-nitro-1,8-naphthalic anhydride (0.2 g, 822 μM) in N,N-dimethylformamide (3 mL), N,N-diethylethylenediamine (0.9 mL, 6.4 mM) was added dropwise at room temperature. The solution was stirred for 8 h at 45 °C, then, the solvent was removed under reduced pressure. Silica gel chromatography (methanol/chloroform, volume ratio 1/30) afforded 0.24 g of **2**. Yield: 70.5%. m.p. 51–52 °C. IR (KBr, cm^{-1}): 3330.8, 2966.3, 2820.4, 1682.5, 1646.5. ^1H NMR ($CDCl_3$, 400 MHz) δ (ppm): 1.11 (m, 6H), 1.13 (m, 6H), 2.65 (m, 4H), 2.69 (m, 4H), 2.80 (t, 2H, J = 12.0 Hz), 2.87 (t, 2H, J = 11.6 Hz), 3.35 (m, 2H), 4.28 (t, 2H, J = 15.6), 6.52 (s, 1H), 6.66 (d, 1H, J = 8.0 Hz), 7.62 (d, 1H, J = 8.8 Hz), 8.09 (d, 1H, J = 8.4 Hz), 8.45 (d, 1H, J = 8.0 Hz), 8.58 (d, 2H, J = 8.0 Hz). ^{13}C NMR ($CDCl_3$, 300 MHz) δ (ppm): 12.24, 12.40, 37.76, 40.17, 46.61, 47.85, 50.06, 50.71, 104.69, 109.90, 120.65, 123.09, 124.84, 126.51, 130.02, 131.24, 134.81, 149.99, 164.33, 164.93. LC-MS: m/z 411.3 $(M+H)^+$. Elemental analysis: $C_{24}H_{34}N_4O_2$ (410.3); Calcd (%): C 70.21, H 8.35, N 13.65, found (%): C 69.14, H 8.22, N 13.38.

3. Materials and methods

The salts used in stock solutions of metal ions were NaCl, KCl, $MgCl_2$, $CaCl_2$, $CrCl_3{\cdot}6H_2O$, $MnSO_4{\cdot}H_2O$, $FeCl_3{\cdot}6H_2O$, $FeCl_2{\cdot}7H_2O$, $CoCl_2{\cdot}6H_2O$, $Ni(NO_3)_2{\cdot}6H_2O$, $CuCl_2{\cdot}2H_2O$, $Zn(NO_3)_2{\cdot}6H_2O$, $CdCl_2{\cdot}2.5H_2O$, $HgCl_2$ and $Pb(NO_3)_2$. Silica gel 60 (200–300 mesh, HaiYang) was used for column chromatography. Analytical thin layer chromatography was performed using YinLong silica gel (precoated sheets, 0.25 mm thick). All the reagents were of analytical grade.

The probes and metal salts were dissolved in water to form 50 mM and 500 mM stock solutions respectively. When examining the fluorescence (FL) response of probes upon protons, 50 μL stock solutions of the probes were diluted to 50 μM with Britton–Robinson buffer at different pH values. When investigating the effect of metal ions on fluorescence of the probes, 50 μL stock solutions of the probes and a few μL stock solutions of metal salts were mixed and diluted with Britton–Robinson buffer. In the detected solutions, the concentration of the probes was 50 μM and the concentration of different metal ions was changed from 500 μM to 10 mM.

IR was recorded on a Nicolet Magan-550 spectrometer. LC–MS was carried out on an Agilent 1200/6220 spectrometer. ^1H NMR and ^{13}C NMR spectra were tested on a Varian Unity Inova spectrometer, operating at 300 MHz and 400 MHz, respectively. The elementary analysis was done on a Carlo-Erba EA1110 CHNO-S. UV–vis spectra were performed on a U-3900 spectrophotometer. Fluorescence spectra were taken on a Fluoromax-4 spectrofluorometer (slit width: 1 nm; T: 25 °C). Fluorescence quantum yield was determined with rhodamine B as a reference (Φ_r = 0.97). pH values were measured on a Mettler-Toledo FE20 pH meter. Melting points were examined by an X-6 micro melting point apparatus.

Cell images were taken on Nikon ECLIPSE TE2000-U Fluorescence Inverted System Microscope. BmN (*Bombyx mori*) insect cells were seeded in a 24-well plate at a density of 5×10^4 cells per well in culture media TC-100 with 10% foetal bovine serum (Sigma) at 27 °C. After 48 h, the cells were separated into four groups and incubated in TC-100, TC-100 with probe **2** (250 μM), TC-100 with probe **2** (250 μM) and HCl (2 mM), TC-100 with probe **2** (250 μM) and NaOH (3 mM) for another 25 min at 27 °C, respectively. After removing most of the media, the cells were imaged on the fluorescence microscope.

Density functional theory (DFT) calculations were performed using the Gaussian 03 program package [51]. The ground-state structure geometries were optimized using Becke's three-parameter hybrid exchange functional with the Lee–Yang–Parr correlation functional (B3LYP) method [52] in conjunction with the 6-31 G(d) basis set [53]. Frequency analysis was employed to identify the structure with the lowest energy.

4. Results and discussion

4.1. Photophysical characteristics of probes *1* and *2*

Probes **1** and **2** are easily dissolved in water and form 50 mM aqueous solutions. Fig. 1 exhibits that two probes have similar absorption and fluorescence (FL) spectra in Britton–Robinson buffer. Mirror symmetry of the fluorescence and absorption spectra in the long-wavelength region indicates the preserved planarity of the probe molecular structure in the exited state [43]. The

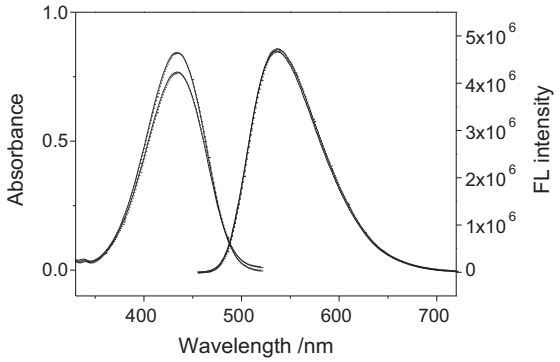

Fig. 1. Absorption and fluorescence spectra of probes **1** and **2** in Britton–Robinson buffer. Top: probe **1**; bottom: probe **2**; c: 50 μM; T: 25 °C; pH = 7.08; λ_{ex} = 434 nm. Slit width: 1 nm.

maximum absorption wavelengths of **1** and **2** are both 434 nm with the molar extinction coefficient 15 400 M^{-1} cm^{-1} for **1** and 16 900 M^{-1} cm^{-1} for **2**. The maximum emission wavelengths are 534 nm with the fluorescence quantum yield 0.524 for **1** and 536 nm with fluorescence quantum yield 0.573 for **2** under the same conditions. The fluorescent quantum yield (Φ_s) of the probe has been calculated using Eq. (1):

$$\Phi_s = \Phi_r \frac{S_s}{S_r} \frac{A_r}{A_s} \frac{n_{Ds}^2}{n_{Dr}^2} \quad (1)$$

where the subscript s and r stand for the sample and reference, respectively. Φ is the emission quantum yields, A represents the absorbance at the excitation wavelength, S refers to the integrated emission band areas and n_D is the solvent refractive index.

4.2. pH sensitivity of probes *1* and *2*

Probes **1** and **2** are sensitive to pH value of the media. Fig. 2 presents their fluorescence spectra in Britton–Robinson buffer at different pH values. It is clear that the fluorescence is on in acidic media and off in alkaline media. When the pH values change from 11.8 to 2.3, the fluorescence enhancement (FE) is 13.6 and 25.6 times for probes **1** and **2**, respectively. Here, the FE was the ratio of maximum fluorescence intensity at pH 2.3 to that at pH 11.8. The changes in the fluorescence intensity as a function of pH are the result of the PET process from the C-4 position peripheral dialkylamino unit to the naphthalimide fluorophore, like other 4-*N*,*N*-dialkylaminoethylamino-*N*-alkyl-1,8-naphthalimides [54–58].

The advantage of introducing dialkylamino unit to imide position lies in the efficient improvement of the probe's water solubility. The good water solubility of the probe makes all detections can be carried out in aqueous media and improves the probe's practicability. Alvino et al. [59] introduced two, three and four dimethylamino (DMA) groups in perylene structure and obtained two water soluble perylene dyes with three and four DMA groups. The UV–vis absorption spectra of the perylene dyes in concentrated hydrochloride aqueous media showed pH-dependent and lost their typical band over 600 nm due to the protonation of the nitrogen atoms, but pH-dependent color changes were not observed in Britton–Robinson buffer of probes **1** and **2**, which is similar to that of Alvino's perylene dye with two DMA groups. Türkmen et al. [60] synthesized a perylene dye with two N,N-dibutylamino groups which could be dissolved in aqueous media as hydrochloride acid. Its fluorescence intensity could be increased by acidic species based on the same PET mechanism as probes **1** and **2**, but all of $ZnCl_2$, Co^{2+} in methanol, acetic acid, TiO_2 or SiO_2 particles could enhance its fluorescence. The FE was about 1.5-fold for the perylene dye with addition of acetic acid. Georgiev et al. [61] reported two tetraester- and PAMAM-branched perylene diimides. The PAMAM-branched dye was water soluble and displayed a good pH sensor activity (FE = 6.4) in water/DMF (1:1, v/v) solution. The tetraester dye could not be dissolved in water, but its pH sensing ability was substantially higher (FE = 184) in water/DMF (1:1, v/v) solution. The two compounds were also sensitive to Cu^{2+}, Pb^{2+} and Fe^{3+} ions in DMF. Our probes **1** and **2** have excellent water solubility and high selectivity and sensitivity to proton in aqueous media within a wide pH range and without any organic solvents, as described in the next section.

The p*K*a values calculated [62,63] according to Fig. 2 are 8.50 for probe **1** and 8.96 for probe **2**, which indicates that **1** and **2** are alkaline and prone to bound protons. Furthermore, the optimized structures of the ground state probe **1** and probe **2** (as shown in Fig. 3) and the Mulliken atomic charges of the structures are calculated by DFT calculation at the B3LYP/6-31G (*d*) level. The Mulliken charges of N19 and N23 atoms linked to the imide side and the 4-position distal end of probe **1** are −0.369572 and −0.368928, respectively, and that of the corresponding N18 and N22 atoms in probe **2** are −0.379851 and −0.379019, respectively. The very close negative charges for N19 and N23, as well as N18 and N22 indicate that both the amino groups in probes **1** and **2** are likely to be protonated at low pH values although the amino group linked to the imide side is a little more basic.

4.3. Selectivity of probes *1* and *2* to various ions

Fig. 4a and b show the selectivity of probes **1** and **2** to various ions, respectively. Upon addition of Na^+, K^+, Mg^{2+}, Ca^{2+}, Cr^{3+}, Mn^{2+}, Fe^{3+}, Fe^{2+}, Co^{2+}, Ni^{2+}, Cu^{2+}, Zn^{2+}, Cd^{2+}, Hg^{2+}, Pb^{2+} (tenfold concentration of the probe) to the 50 μM probe solutions, no significant

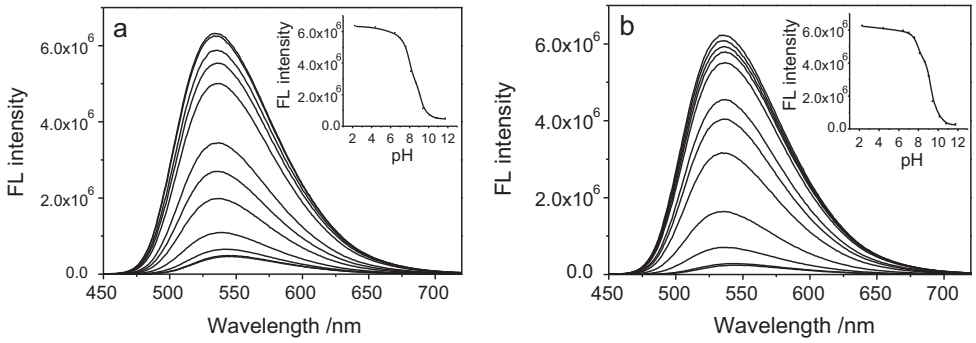

Fig. 2. Fluorescence response of probes **1** and **2** upon different pH values in Britton–Robinson buffer. Inset: plot of fluorescence intensity depending on the pH values (excitation at 434 nm, 25 °C). (a) Probe **1** (50 μM), from top to bottom, pH: 2.30, 4.47, 6.51, 7.09, 7.67, 8.19, 8.71, 9.09, 9.46, 10.17, 10.87, 11.81. (b) Probe **2** (50 μM), from top to bottom, pH: 2.33, 4.50, 6.50, 7.08, 7.66, 8.18, 8.72, 9.10, 9.48, 10.19, 10.89, 11.82.

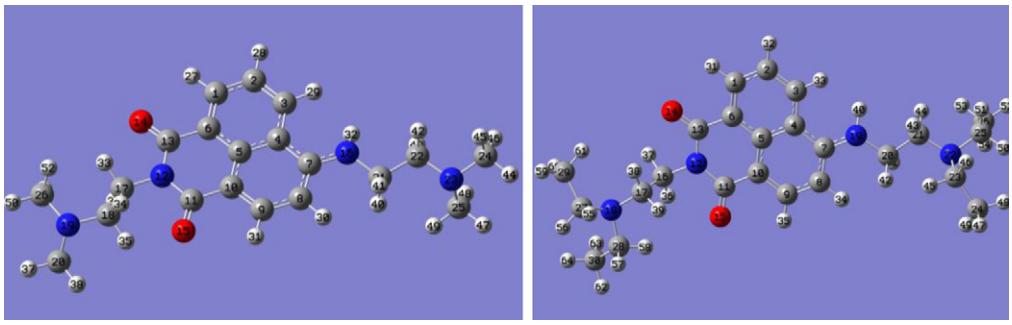

Fig. 3. Structure of the ground state probe **1** and probe **2**. Grey, silvery, blue and red circles represent carbon, hydrogen, nitrogen and oxygen atoms, respectively. (For interpretation of color mentioned in this figure legend the reader is referred to the web version of the article.)

fluorescence intensity changes were observed. However, the same amount of H^+ led to a remarkable enhancement in fluorescence intensity, and the fluorescence intensity changes caused by H^+ are not obviously influenced by the coexisting Na^+, K^+ (10 mM), Mg^{2+}, Ca^{2+} (5 mM), Cr^{3+}, Mn^{2+}, Fe^{3+}, Fe^{2+}, Co^{2+}, Ni^{2+}, Cu^{2+}, Zn^{2+}, Cd^{2+}, Hg^{2+}, Pb^{2+} (500 μM), Cl^- (28 mM), PO_4^{3-} (40 mM), SO_4^{2-} (500 μM), NO_3^- (3 mM) at pH 6.59, 7.17 and 7.74, which can be seen from Fig. 4c. The results indicate that probes **1** and **2** have high selectivity to protons in Britton–Robinson buffer. Furthermore, probe **1** is more sensitive to H^+ than probe **2**, as presented in Fig. 4a and b, while probe **2** is less affected by the coexisting ions, as shown in Fig. 4c.

4.4. Living cell imaging with probes *1* and *2*

We choose probe **2** which is less disturbed by the other ions to explore its applications in bioimaging. The situation was that the *Bombyx mori* (BmN) cells cultured in the media without probe **2** at pH 6.24 were invisible under excitation, the cells incubated in the media with probe **2** (250 μM) at pH 6.47 exhibited green fluorescence, the cells cultured in the media with probe **2** (250 μM) and HCl (2 mM) at pH 5.51 exhibited weak green fluorescence, while the cells incubated in the media with probe **2** (250 μM) and NaOH (3 mM) at pH 7.55 emitted strong green fluorescence (presented in Fig. 5). It is clear that the fluorescence intensity of the cells increased when the pH_e of the **2**-containing culture media increased from 5.51 to 7.55. The fact that the higher the pH_e is, the brighter the cells become indicates that probe **2** can provide pH_e information for studying physiological and pathological processes.

The proposed mechanism for the cell fluorescence off–on from low pH_e to high pH_e may be explained as follows: probe **2**, HCl and NaOH are in the culture media and they mainly influence the extracelluar pH (pH_e) since living cells have excellent ability to keep intracellular pH_i stable by ion transport systems in the cell membrane and high buffering capacity of the cytoplasm [64]. The fluorescence of probe **2** can be displayed in the culture media or the cell, which is determined by the pH (pH_e and pH_i), and the cell-membrane penetrating ability of the probe and the protonated probe. The changes of cell image fluorescence mainly result from the amount of probe **2** entrapped and protonated by the cells. According to the fluorescence data given above, low pH will cause strong fluorescence. When the pH_e of the culture media is low,

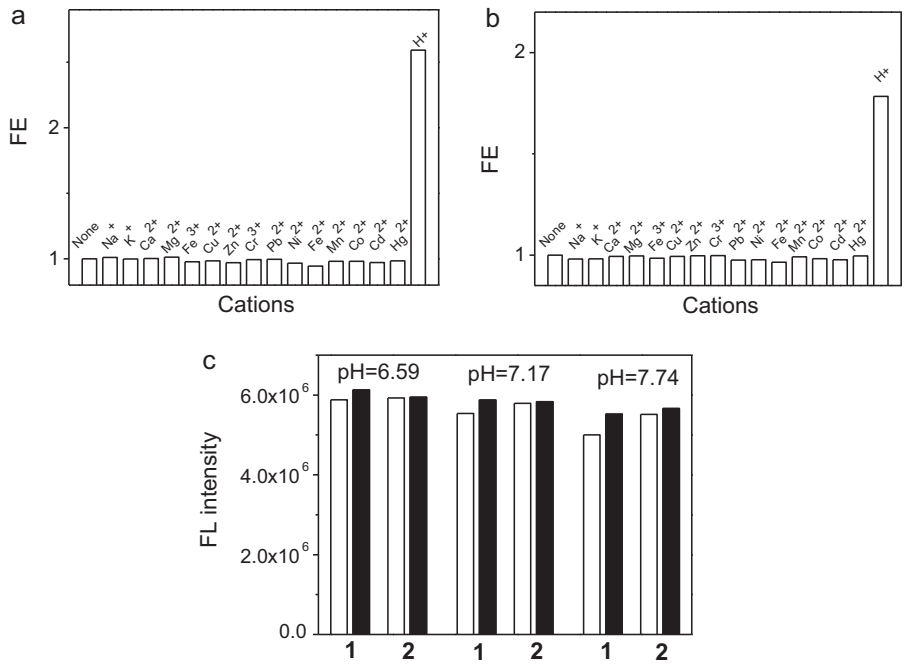

Fig. 4. Fluorescence responses of **1** and **2** in the presence of different ions in Britton–Robinson buffer (excitation at 434 nm, emission at 534 nm for **1** and 536 nm for **2**). (a) and (b) Fluorescence enhancement (FE) of **1** and **2** (50 μM) caused by different ions (500 μM). (c) Fluorescence maxima of **1** and **2** (50 μM) at different pH. White column: without extraneous ions; black column: with Na^+, K^+ (10 mM), Mg^{2+}, Ca^{2+} (5 mM), Cr^{3+}, Mn^{2+}, Fe^{3+}, Fe^{2+}, Co^{2+}, Ni^{2+}, Cu^{2+}, Zn^{2+}, Cd^{2+}, Hg^{2+}, Pb^{2+} (500 μM), Cl^- (28 mM), PO_4^{3-} (40 mM), SO_4^{2-} (500 μM), NO_3^- (3 mM).

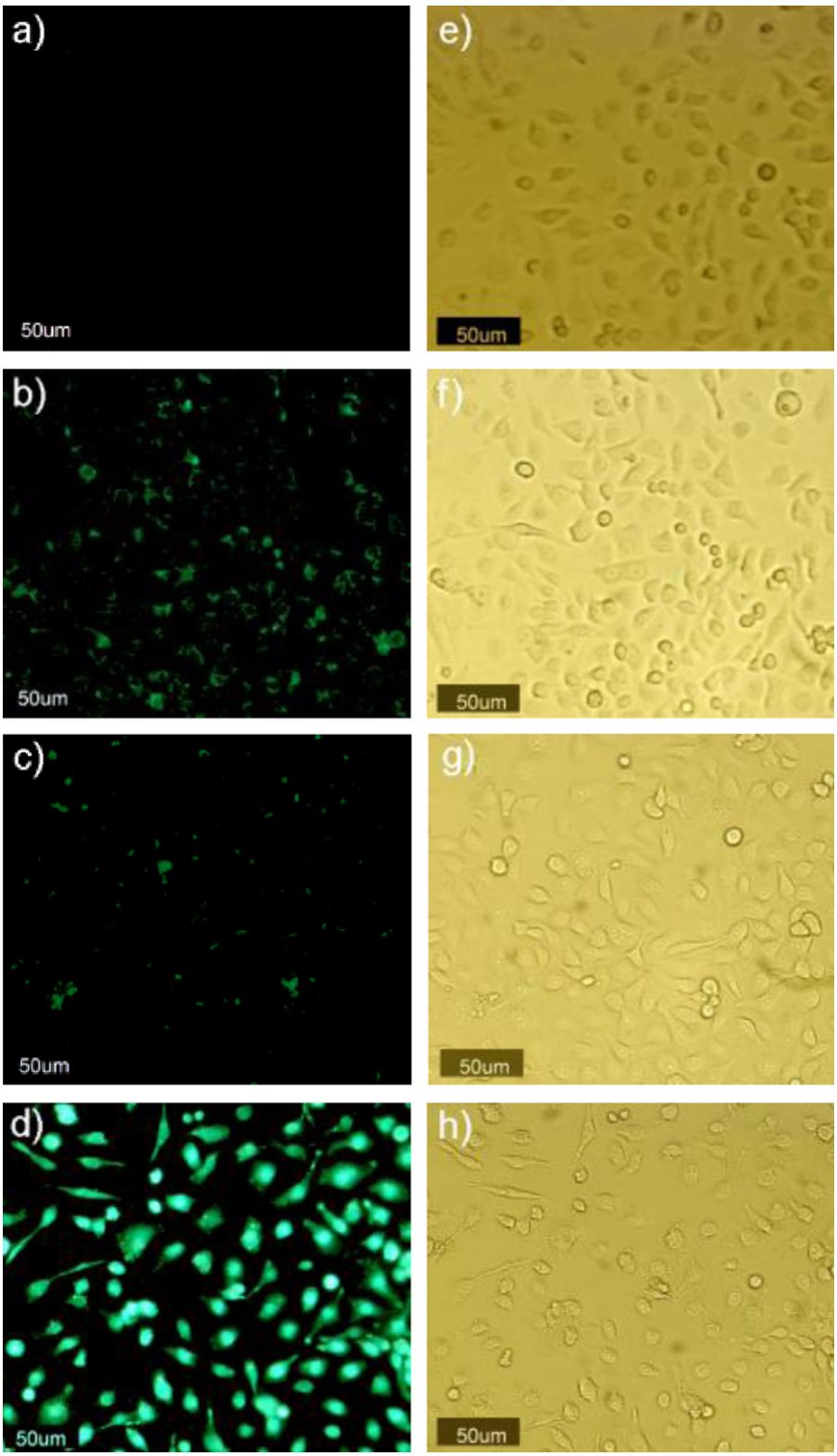

Fig. 5. Images of BmN cells incubated in different pH_e media. (a)–(d) Fluorescence images: (a) without probe **2** at pH_e 6.24; (b) with probe **2** (250 μM) at pH_e 6.47; (c) with probe **2** (250 μM) and HCl (2 mM) at pH_e 5.51; (d) with probe **2** (250 μM) and NaOH (3 mM) at pH_e 7.55. (e)–(h) are corresponding microscopic images of (a)–(d), respectively. Color figures can be viewed in the online issue, which is available at http://ees.elsevier.com/jphotochem/.

the probe molecules are primary protonated by the extracelluar H^+ and elicit high fluorescence in culture media. The charged probe molecules have poor cell membrane permeability so that only the very few rest of nonprotonated probe molecules can enter into the cells, protonated by the intracellular H^+ and result in very weak cell fluorescence. The cell fluorescence increases while the culture-media fluorescence decreases along with the pH_e rises. When the cells were exposed to the high-pH_e culture media, the H^+ in the culture media was not enough to protonate the probe, a large number of probe molecules entered into the cells and accumulated inside

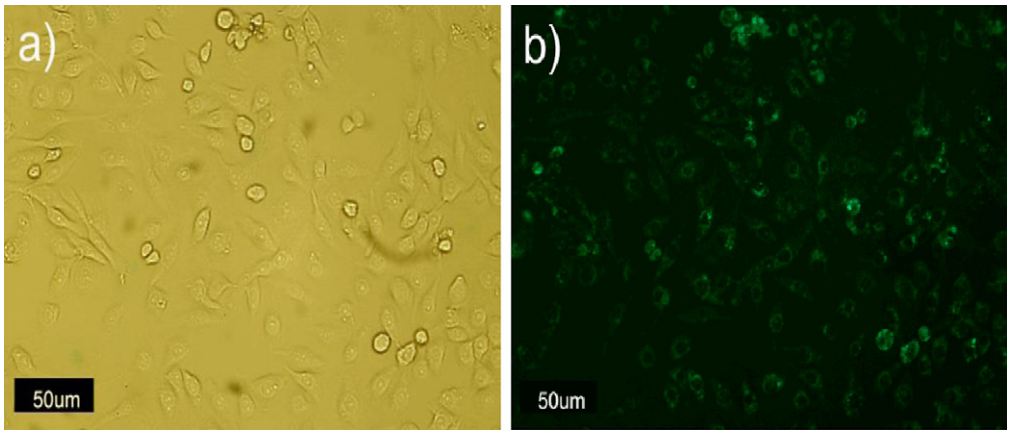

Fig. 6. Images of BmN cells incubated in media with probe **2** (150 μM) at pH_e 6.36: (a) microscopic images and (b) fluorescence images. Color figures can be viewed in the online issue, which is available at http://ees.elsevier.com/jphotochem/.

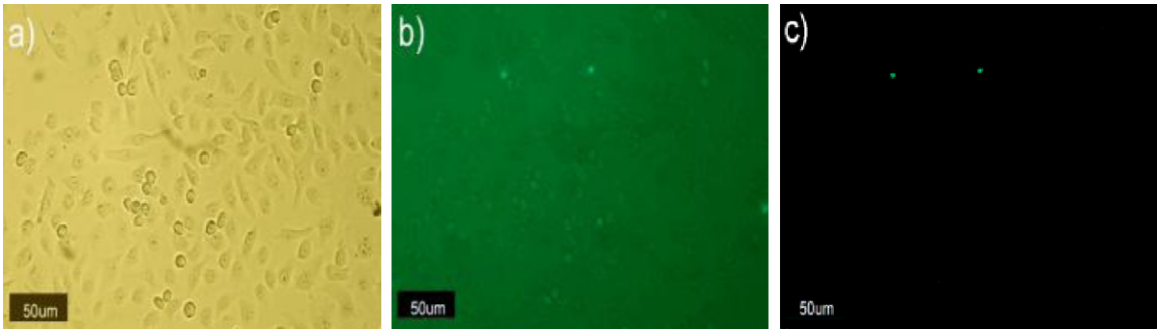

Fig. 7. Images of BmN cells incubated in media with probe **2** (250 μM) and HCl (8 mM) at pH_e 4.63: (a) microscopic images; (b) and (c) fluorescence images before and after removing the culture media, respectively. Color figures can be viewed in the online issue, which is available at http://ees.elsevier.com/jphotochem/.

cells due to relative low intracellular pH_i, leading to dark culture-media image and bright cell fluorescent image.

Fig. 5a and b can prove the cell-membrane permeability of probe **2** because cells cultured without probe **2** at pH_e 6.24 were invisible and cells cultured with probe **2** at pH_e 6.47 emitted green fluorescence under excitation. The results reveal that the probe can penetrate the cell membrane, enter into the cells, be protonated by the intracellular H^+ and illumine the cells. Moreover, to investigate if the dye molecules can be internalized and entrapped in the highly acidic endolysosomal pathway, we incubated the cells in media with lower concentration (150 μM compared to 250 μM) probe **2** at lower pH_e (6.36 compared to 6.47) in order to make fewer probe into the cell. The results show that the fluorescence of probe **2** is observed inside the cells, and the probe seems to enrich in some places in the cytoplasm which may be low pH organelle such as lysosome, as shown in Fig. 6b.

To support the supposition that the protonated probe molecules have poor cell membrane permeability, the cells were incubated in media with probe **2** (250 μM) and HCl (8 mM) at pH 4.63 (It is the pH_e). It can be seen that the culture medium emits high fluorescence so that the cells in it almost could not be seen, as shown in Fig. 7b, which implies that probe **2** was protonated and aggregated outside cells where the pH was low. After removing the culture medium, the cell images are nearly dark, as exhibited in Fig. 7c, which indicates that the charged probe **2** has poor cell-membrane permeability and could not internalized by the cells.

Overall, the cell membrane was permeable to the neutral dye molecules but not to the protonated dye ones, the positive charges of the protonated amino groups prohibit the probe across the cell membrane. This phenomenon is similar to the literature result that the esterified version of the neutral probe is cell-membrane permeable until cytosolic esterases cleave the ester to yield a carboxylic acid and carboxylic acid is deprotonated, the negative charges of the deprotonated carboxylates deprive the probe of its cell-membrane permeability [65,66].

5. Conclusions

Two water soluble 1,8-naphthalimide derivates have been reported. They are highly selective to protons and can be used as fluorescent pH probes. All detections can be carried out in aqueous media and a large number of biologically relevant ions showed no obvious interferences with the detection. The results from living cell image indicate that the synthesized compounds can permeate cell membrane and have potential applications in biological systems.

Acknowledgment

This work is funded by the National Natural Science Foundation of China (21074085), the Open Research Foundation of the National Engineering Laboratory for Modern Silk, Soochow University (SS115801) and the Open Research Foundation of the Key Laboratory of Organic Synthesis of Jiangsu Province, Soochow University (KJS0911).

References

[1] B. Tang, F. Yu, P. Li, L. Tong, X. Duan, T. Xie, X. Wang, A near-infrared neutral pH fluorescent probe for monitoring minor pH changes: imaging in living HepG2 and HL-7702 cells, J. Am. Chem. Soc. 131 (2009) 3016–3023.
[2] J. Han, K. Burgess, Fluorescent indicators for intracellular pH, Chem. Rev. 110 (2010) 2709–2728.

[3] Q. Jia, C. Wang, X. Du, F. Li, H. Zhang, Modulation of KCNQ2 and KCNQ3 potassium channels by extracellular pH, Chin. Pharm. Acolog. Bull. 21 (2005) 82–87.
[4] J. Ma, A. Luo, W. Wang, P. Zhang, Low extracellular pH increases the persistent sodium current in guinea pig ventricular myocytes, Acta Physiol. Sin. 59 (2007) 233–239.
[5] C. Hille, M. Berg, L. Bressel, D. Munzke, P. Primus, H. Löhmannsröben, C. Dosche, Time-domain fluorescence lifetime imaging for intracellular pH sensing in living tissues, Anal. Bioanal. Chem. 391 (2008) 1871–1879.
[6] K.M. Sun, C.K. McLaughlin, D.R. Lantero, R.A. Manderville, Biomarkers for phenol carcinogen exposure act as pH-sensing fluorescent probes, J. Am. Chem. Soc. 129 (2007) 1894–1895.
[7] S. Charier, O. Ruel, J. Baudin, D. Alcor, J. Allemand, A. Meglio, L. Jullien, An efficient fluorescent probe for ratiometric pH measurements in aqueous solutions, Angew. Chem. Int. Ed. 43 (2004) 4785–4788.
[8] S. Charier, O. Ruel, J. Baudin, D. Alcor, J. Allemand, A. Meglio, L. Jullien, B. Valeur, Photophysics of a series of efficient fluorescent pH probes for dual emission-wavelength measurements in aqueous solutions, Chem. Eur. J. 12 (2006) 1097–1113.
[9] T.J. Rink, R.Y. Tsien, T. Pozzan, Cytoplasmic pH and free Mg^{2+} in lymphocytes, J. Cell Biol. 95 (1982) 189–196.
[10] J. Li, S.Q. Yao, Singapore green: a new fluorescent dye for microarray and bioimaging applications, Org. Lett. 11 (2009) 405–408.
[11] A. Unciti-Broceta, M. Rahimi Yusop, P.R. Richardson, J.G.A. Walton, M. Bradley, A fluorescein-derived anthocyanidin-inspired pH sensor, Tetrahedron Lett. 50 (2009) 3713–3715.
[12] R. P. Haugland, J. Whitaker, (Molecular Probes, Inc.), Xanthene dyes having a fused (C) benzo ring, U.S. Patent Application US 4,945,171 (1990).
[13] N. Marcotte, A.M. Brouwer, Carboxy, SNARF-4F as a fluorescent pH probe for ensemble and fluorescence correlation spectroscopies, J. Phys. Chem. B 109 (2005) 11819–11828.
[14] Y.M. Cheng, T. Kelly, J. Church, Potential contribution of a voltage-activated proton conductance to acid extrusion from rat hippocampal neurons, Neuroscience 151 (2008) 1084–1098.
[15] Z. Li, C. Niu, G. Zeng, Y. Liu, P. Gao, G. Huang, Y. Mao, A novel fluorescence ratiometric pH sensor based on covalently immobilized piperazinyl-1,8-napthalimide and benzothioxanthene, Sensor. Actuat. B 114 (2006) 308–315.
[16] Z. Xu, X. Qian, J. Cui, R. Zhang, Exploiting the deprotonation mechanism for the design of ratiometric and colorimetric Zn^{2+} fluorescent chemosensor with a large red-shift in emission, Tetrahedron 62 (2006) 10117–10122.
[17] H. Lu, X. Bin, Y. Dong, F. Chen, Y. Li, Z. Li, J. He, H. Li, W. Tian, Novel fluorescent pH sensors and a biological probe based on anthracene derivatives with aggregation-induced emission characteristics, Langmuir 26 (2010) 6838–6844.
[18] P. Rohrbach, O. Friedrich, J. Hentschel, H. Plattner, R.H.A. Fink, M. Lanzer, Quantitative calcium measurements in subcellular compartments of plasmodium falciparum-infected erythrocytes, J. Biol. Chem. 280 (2005) 27960–27969.
[19] F. Galindo, M.I. Burguete, L. Vigara, S.V. Luis, N. Kabir, J. Gavrilovic, D.A. Russell, Synthetic macrocyclic peptidomimetics as tunable pH probes for the fluorescence imaging of acidic organelles in live cells, Angew. Chem. Int. Ed. 44 (2005) 6504–6508.
[20] T. Myochin, K. Kiyose, K. Hanaoka, H. Kojima, T. Terai, T. Nagano, Rational design of ratiometric near-infrared fluorescent pH probes with various pK_a values, based on aminocyanine, J. Am. Chem. Soc. 133 (2011) 3401–3409.
[21] Y. Xu, Y. Liu, X. Qian, Novel cyanine dyes as fluorescent pH sensors: PET, ICT mechanism or resonance effect? J. Photochem. Photobiol. A: Chem. 190 (2007) 1–8.
[22] B. Wang, L. Wang, T. Wu, Z. Yang, X. Peng, Synthesis of pH probe based on styrylcyanine dyes and fluorescence image in live cell, Chem. J. Chinese U. 31 (2010) 1148–1151.
[23] Z. Zhang, S. Achilefu, Design, synthesis and evaluation of near-infrared fluorescent pH indicators in a physiologically relevant range, Chem. Commun. (2005) 5887–5889.
[24] B. Tang, X. Liu, K. Xu, H. Huang, G. Yang, L. An, A dual near-infrared pH fluorescent probe and its application in imaging of HepG2 cells, Chem. Commun. (2007) 3726–3728.
[25] J. Murtagh, D.O. Frimannsson, D.F. O'Shea, Azide conjugatable and pH responsive near-infrared fluorescent imaging probes, Org. Lett. 11 (2009) 5386–5389.
[26] M. Tian, X. Peng, F. Feng, S. Meng, J. Fan, S. Sun, Fluorescent pH probes based on boron dipyrromethene dyes, Dyes Pigments 81 (2009) 58–62.
[27] M. Baruah, W. Qin, N. Basaric, W. De Borggraeve, N. Boens, BODIPY-based hydroxyaryl derivatives as fluorescent pH probes, J. Org. Chem. 70 (2005) 4152–4157.
[28] T. Yogo, Y. Urano, A. Mizushima, H. Sunahara, T. Inoue, K. Hirose, M. Lino, K. Kikuchi, T. Nagano, Selective photoinactivation of protein function through environment-sensitive switching of singlet oxygen generation by photosensitizer, Proc. Natl. Acad. Sci. U.S.A. 105 (2008) 28–32.
[29] Q.A. Best, R. Xu, M.E. McCarroll, L. Wang, D.J. Dyer, Design and investigation of a series of rhodamine-based fluorescent probes for optical measurements of pH, Org. Lett. 12 (2010) 3219–3221.
[30] X. Wan, D. Wang, S. Liu, Fluorescent pH-sensing organic/inorganic hybrid mesoporous silica nanoparticles with tunable redox-responsive release capability, Langmuir 6 (2010) 15574–15579.
[31] S.A. Hilderbrand, K.A. Kelly, M. Niedre, R. Weissleder, Near infrared fluorescence-based bacteriophage particles for ratiometric pH imaging, Bioconjugate Chem. 19 (2008) 1635–1639.
[32] V. Biju, T. Itoh, M. Ishikawa, Delivering quantum dots to cells: bioconjugated quantum dots for targeted and nonspecific extracellular and intracellular imaging, Chem. Soc. Rev. 39 (2010) 3031–3056.
[33] D. Staneva, M. McKena, P. Bosch, I. Grabchev, Synthesis and spectroscopic studies of a new 1,8-naphthalimide dyad as detector for metal cations and protons, Spectrochim. Acta A 76 (2010) 150–154.
[34] I. Grabchev, S. Dumas, J. Chovelon, A. Nedelcheva, First generation poly(propyleneimine) dendrimers functionalised with 1,8-naphthalimide units as fluorescence sensors for metal cations and protons, Tetrahedron 64 (2008) 2113–2119.
[35] Z. Xu, X. Qian, J. Cui, Colorimetric and ratiometric fluorescent chemosensor with a large red-shift in emission: Cu(II)-only sensing by deprotonation of secondary amines as receptor conjugated to naphthalimide fluorophore, Org. Lett. 7 (2005) 3029–3032.
[36] D. Cui, X. Qian, F. Liu, R. Zhang, Novel fluorescent pH sensors based on intramolecular hydrogen bonding ability of naphthalimide, Org. Lett. 6 (2004) 2757–2760.
[37] J. Fan, X. Peng, Y. Wu, E. Lu, J. Hou, H. Zhang, R. Zhang, X. Fu, A new PET fluorescent sensor for Zn^{2+}, J. Lumin. 114 (2005) 125–130.
[38] L. Cui, Y. Zhong, W. Zhu, Y. Xu, Q. Du, X. Wang, X. Qian, Y. Xiao, A new prodrug-derived ratiometric fluorescent probe for hypoxia: high selectivity of nitroreductase and imaging in tumor cell, Org. Lett. 13 (2011) 928–931.
[39] J.F. Zhang, C.S. Lim, S. Bhuniya, B.R. Cho, J.S. Kim, A highly selective colorimetric and ratiometric two-photon fluorescent probe for fluoride ion detection, Org. Lett. 13 (2011) 1190–1193.
[40] V.B. Bojinov, N.I. Georgiev, N.V. Marinova, Design and synthesis of highly photostable fluorescence sensing 1,8-naphthalimide-based dyes containing s-triazine UV absorber and HALS units, Sensor. Actuat. B 148 (2010) 6–16.
[41] V.B. Bojinov, I.P. Panova, Novel 4-(2,2,6,6-tetramethylpiperidin-4-ylamino)-1,8-naphthalimide based yellow-green emitting fluorescence sensors for transition metal ions and protons, Dyes Pigments 80 (2009) 61–66.
[42] H. Lin, P. Herman, J.S. Kang, J.R. Lakowicz, Fluorescence lifetime characterization of novel low-pH probes, Anal. Biochem. 294 (2001) 118–125.
[43] D. Staneva, I. Grabchev, J. Soumillion, V.B. Bojinov, A new fluorosensor based on bis-1,8-naphthalimide for metal cations and protons, J. Photochem. Photobiol. A: Chem. 189 (2007) 192–197.
[44] I. Grabchev, X. Qian, V.B. Bojinov, Y. Xiao, W. Zhang, Synthesis and photophysical properties of 1,8-naphthalimide-labelled PAMAM as PET sensors of protons and of transition metal ions, Polymer 43 (2002) 5731–5736.
[45] S. Salia, I. Grabchev, J. Chovelon, G. Ivanova, Selective sensors for Zn^{2+} cations based on new green fluorescent poly(amidoamine) dendrimers peripherally modified with 1,8-naphthalimides, Spectrochim. Acta A 65 (2006) 591–597.
[46] I. Grabchev, S. Guittonneau, Sensors for detecting metal ions and protons based on new green fluorescent poly(amidoamine) dendrimers peripherally modified with 1,8-naphthalimides, J. Photochem. Photobiol. A: Chem. 179 (2006) 28–34.
[47] I. Grabchev, P. Bosch, M. McKenna, A. Nedelcheva, Synthesis and spectral properties of new green fluorescent poly(propyleneimine) dendrimers modified with 1,8-naphthalimide as sensors for metal cations, Polymer 48 (2007) 6755–6762.
[48] L.A. Jones, C.T. Joyner, H.K. Kim, R.A. Kyff, Acenaphthene I. The preparation of derivatives of 4,5-diamino naphthalic anhydride, Can. J. Chem. 48 (1970) 3132–3135.
[49] I. Antonini, R. Volpini, D.D. Ben, C. Lambertucci, G. Cristalli, Design, synthesis, and biological evaluation of new mitonafide derivatives as potential antitumor drugs, Bioorgan. Med. Chem. 16 (2008) 8440–8446.
[50] J. Zhang, R.J. Woods, P.B. Brown, R.A. Mowery, R.R. Kane, W. Robert, R.W. Jackson, F. Pollo, Photochemical tissue bonding using monomeric 4-amino-1,8-naphthalimides, J. Biomed. Opt. 9 (2004) 1089–1092.
[51] M.J. Frisch, G.W. Trucks, H.B. Schlegel, G.E. Scuseria, M.A. Robb, J.R. Cheeseman, J.A. Montgomery Jr., T. Vreven, K.N. Kudin, J.C. Burant, J.M. Millam, S.S. Iyengar, J. Tomasi, V. Barone, B. Mennucci, M. Cossi, G. Scalmani, N. Rega, G.A. Petersson, H. Nakatsuji, M. Hada, M. Ehara, K. Toyota, R. Fukuda, J. Hasegawa, M. Ishida, T. Nakajima, Y. Honda, O. Kitao, H. Nakai, M. Klene, X. Li, J.E. Knox, H.P. Hratchian, J.B. Cross, V. Bakken, C. Adamo, J. Jaramillo, R. Gomperts, R.E. Stratmann, O. Yazyev, A.J. Austin, R. Cammi, C. Pomelli, J.W. Ochterski, P.Y. Ayala, K. Morokuma, G.A. Voth, P. Salvador, J.J. Dannenberg, V.G. Zakrzewski, S. Dapprich, A.D. Daniels, M.C. Strain, O. Farkas, D.K. Malick, A.D. Rabuck, K. Raghavachari, J.B. Foresman, J.V. Ortiz, Q. Cui, A.G. Baboul, S. Clifford, J. Cioslowski, B.B. Stefanov, G. Liu, A. Liashenko, P. Piskorz, I. Komaromi, R.L. Martin, D.J. Fox, T. Keith, M.A. Al-Laham, C.Y. Peng, A. Nanayakkara, M. Challacombe, P.M.W. Gill, B. Johnson, W. Chen, M.W. Wong, C. Gonzalez, J.A. Pople, Gaussian 03 Rev. C2, Gaussian, Inc., Pittsburgh, PA, 2004.
[52] A.D. Becke, Density-functional thermochemistry. III. The role of exact exchange, J. Chem. Phys. 98 (1993) 5648–5652.
[53] M.M. Francl, W.J. Pietro, W.J. Hehre, J.S. Binkley, M.S. Gordon, D.J. Defrees, J.A. Pople, Self-consistent molecular orbital methods. XXIII. A polarization-type basis set for second-row elements, J. Chem. Phys. 77 (1982) 3654–3665.
[54] A.P. de Silva, H.Q.N. Gunaratne, J. Habib Jiwan, C.P. McCoy, T.E. Rice, J. Soumillion, New fluorescent model compounds for the study of photoinduced electron transfer: the influence of molecular electric field in the excited state, Angew. Chem. Int. Ed. 34 (1995) 1728–1731.
[55] A.P. de Silva, T.E. Rice, A small supramolecular system which emulates the unidirectional, path-selective photoinduced electron transfer (PET) of the bacterial photosynthetic reaction centre (PRC), Chem. Commun. 163 (1999) 163–164.

[56] V.B. Bojinov, T.N. Konstantinova, Fluorescent 4-(2,2,6,6-tetramethylpiperidin-4-ylamino)-1,8-naphthalimide pH chemosensor based on photoinduced electron transfer, Sensor. Actuat. B 123 (2007) 869–876.
[57] V.B. Bojinov, D.B. Simeonov, N.I. Georgiev, A novel blue fluorescent 4-(1,2,2,6,6-pentamethylpiperidin-4-yloxy)-1,8-naphthalimide pH chemosensor based on photoinduced electron transfer, Dyes Pigments 76 (2008) 41–46.
[58] V.B. Bojinov, I.P. Panova, J. Chovelon, Novel blue emitting tetra- and pentamethylpiperidin-4-yloxy-1,8-naphthalimides as photoinduced electron transfer based sensors for transition metal ions and protons, Sensor. Actuat. B 135 (2008) 172–180.
[59] A. Alvino, M. Franceschin, C. Cefaro, S. Borioni, G. Ortaggi, A. Bianco, Synthesis and spectroscopic properties of highly water-soluble perylene derivatives, Tetrahedron 63 (2007) 7858–7865.
[60] G. Türkmen, S. Erten-Ela, S. Icli, Highly soluble perylene dyes: synthesis, photophysical and electrochemical characterizations, Dyes Pigments 83 (2009) 297–303.
[61] N.I. Georgiev, A.R. Sakr, V.B. Bojinov, Design and synthesis of novel fluorescence sensing perylene diimides based on photoinduced electron transfer, Dyes Pigments 91 (2011) 332–339.
[62] R.A. Bissell, A.P. de Silva, H.Q.N. Gunaratne, P.L.M. Lynch, G.E.M. Maguire, K.R.A.S. Sandanayake, Molecular fluorescent signalling with 'fluor–spacer–receptor' systems: approaches to sensing and switching devices via supramolecular photophysics, Chem. Soc. Rev. 21 (1992) 187–195.
[63] I. Grabchev, D. Staneva, J. Chovelon, Photophysical investigations on the sensor potential of novel, poly(propylenamine) dendrimers modified with 1,8-naphthalimide units, Dyes Pigments 85 (2010) 189–193.
[64] Z. Qing, L. Linsheng, X. Jun, Jujube date polysaccharide can increase pH in murine peritoneal macrophages, Pharmacol. Clin. Chin. Mat. Med. 18 (2002) 8–9.
[65] L.E. McQuade, S.J. Lippard, Cell-trappable quinoline-derivatized fluoresceins for selective and reversible biological Zn(ii) detection, Inorg. Chem. 49 (2010) 9535–9545.
[66] M.D. Pluth, L.E. McQuade, S.J. Lippard, Cell-trappable fluorescent probes for nitric oxide visualization in living cells, Org. Lett. 12 (2010) 2318–2321.